Strong Enhancements in Output Power and High-Speed Data Transmission Performances by Using Parallel Oxide-Relief/Zn-Diffusion 850 nm VCSELs

Kai-Lun Chi[1], Xin-Nan Chen[1], Jye-Hong Chen[2], J. E. Bowers[3], and Ying-Jay Yang[4], and Jin-Wei Shi[1*]
[1]Department of Electrical Engineering, National Central University, Taoyuan 320, Tawian
*Tel: +886-3-4227151 ext. 34466, *FAX: +886-3-4255830, *Email: jwshi@ee.ncu.edu.tw
[2]Department of Photonics, National Chiao-Tung University, Hsinchu 300, Taiwan
[3]Department of Electrical and Computer Engineering, University of California Santa Barbara, CA, 93106.
[4]Department of Electrical Engineering, National Taiwan University, Taipei, 106, Taiwan

Abstract: By using parallel two high-speed VCSELs, double increase in maximum output power (4 vs. 8mW), negligible degradation in 3-dB electrical-to-optical bandwidth (~25 GHz), and strong enhancement in 46 Gbit/sec data transmission through OM4 MMF is achieved compared with those of single reference.

I. Introduction

Vertical-cavity surface-emitting lasers (VCSELs) with central wavelength at 850 nm has become the most important light source in the booming market of short-reach (< 300 meters) optical interconnect (OI). The next generation interconnect framework has been targeted at data rate per channel as high as 56 Gbit/sec (CEI (Common Electrical Interface)-56G) [1-3] with the total data rate up to 400 Gbit/sec. The complex modulation/de-modulation techniques, such as pulse-amplitude modulation (PAM) [4] and feed forward equalizations (FFEs) has been demonstrated to release the bottleneck of speed of 850 nm VCSEL under direct modulation. However, by use of the above-mentioned techniques to boost the data rate, the power budget in the linking channel becomes more critical [4]. To have several VCSELs in parallel as high-power and high-speed VCSEL array [5] is one of the promising solutions to further increase the total output power during high-speed modulation. However, the degradation in modulation speed of parallel VCSEL as compared to that of single one is usually observed due to the increase in parasitic capacitance of array. In this work, we demonstrate a novel VCSEL array structure, which can greatly release the trade-off among modulation speed and maximum output power. By using unit VCSEL with Zn-diffusion and oxide-relief apertures [3], the differential resistance and parasitic capacitance can be significantly reduced, respectively. In addition, thanks to the Zn-diffusion aperture in our unit VCSEL, the increasing in coupling loss between array output and MMF can be avoided. Compared with reference VCSEL unit, the two-unit parallel array shows an two times improvement in maximum output power (8 vs. 4 mW), the same 3-dB E-O bandwidth (~25 GHz), and enhancement in error-free data rate (46 vs. 44 GHz) through OM4 MMF.

II. Device Structure

Figures 1 (a) and (b) shows the top-view of demonstrated single reference VCSEL and two-unit VCSEL array, respectively. The conceptual cross-sectional view of the unit VCSEL is given in Figure 2 (a). As shown in Figure 1, the fabricated device has a ~23 μm diameter active mesa, which is integrated with the slot line pads for on-wafer high-speed measurement. In order to collect the output light by use of the MMF with a 50 μm core diameter, the spacing between the centers of neighboring light-emission aperture in our array is set as close as possible, which is around 34 μm, as specified in Figure 1 (b). As shown in Figure 2 (a), with additional Zn-diffusion apertures in the top p-type DBR layers, we can not only manipulate the optical far-field patterns but also reduce the differential resistance [3]. In addition, the oxide-relief aperture in our structure can further reduce the parasitic capacitance of VCSEL [3]. Here, such unique structure should be the key to minimize the degradation in RC-limited bandwidth of our parallel VCSEL array. The value of its total parasitic capacitance is linear proportional to the number of parallel units and capacitance of each single device. The diameters of the Zn-diffusion (W_Z) and oxide-relief apertures (W_o) and Zn-diffusion depths (d) of measured devices is 8, 4, and 1 μm, respectively, as specified on Figure 2 (a). The detail of epi-layer structure and device fabrication processes can be referred to our previous work [3].

III.Measurement Results

The free-space light output power and bias voltages versus current (L-I and V-I) characteristics of single reference (devices A and B) and two-units parallel array (devices C and D) is shown in Figure 2 (b). As can be seen, the maximum output power of parallel array is over twice larger than that of the single reference and with only ~1.6 times of threshold current (0.9 vs. 1.5 mA). Furthermore, the differential resistance of array can be significantly reduced from 57 to 38 Ω due to parallel connection. Figure 2 (c) shows the measured output optical spectra of single device and parallel array under different bias currents. The insets in such Figure show the corresponding measured 2-D far-field patterns of each device. Thanks to the Zn-diffusion apertures in our devices, their far-field pattern is single spot and very similar, which implies that the coupling loss from the parallel array output into MMF would not further increase as compared to that of a single device. Figure 3 (a) and (b) shows the measured E-O frequency responses under different bias currents of device A and D, respectively. We can clearly see that both structures have the same maximum 3-dB E-O bandwidth at around 25 GHz. Such result indicates that the RC-limited bandwidth should not be the dominant speed limiting factor in their net E-O bandwidths. In order to investigate the RC-limited frequency response, the equivalent-circuit modeling technique was performed onto our

devices. Figure 4 (a) shows the adopted equivalent circuit model and (b) shows the measured and fitted microwave reflection coefficients (S_{11}) of device A and D. We can clearly see that the measured and fitted traces from near dc to 30 GHz match very well. According to the extracted values of circuit elements used for fitting process, the RC-limited frequency response of device A and D can then be determined, as shown in Figure 4 (c). The extracted RC-limited 3-dB bandwidths of both devices is much higher than that of net E-O bandwidth (>50 vs. 25 GHz), as expected. Figure 5 (a) and (b) shows the measured error-free eye-patterns of device A and D at 44 and 46 Gbit/sec data rate, respectively. The length of OM4 MMF used for data transmission in both cases is the same as around 10 meter. By further increasing the bias current (12 vs. 6 mA) in device D with a larger optical modulation amplitude, the superior transmission performance at a higher data rate (46 vs. 44Gbit/sec) than those of device A is achieved.

IV. Summary

In conclusion, by utilizing the Zn-diffusion and oxide-relief apertures in our parallel VCSEL array, a higher maximum output power can be achieved without sacrificing its 3-dB O-E bandwidth (~25 GHz) as compared to those of single reference. Significant improvement in transmission performance at data rate as high as 46 Gbit/sec has been successfully achieved through the use of demonstrated 2-unit parallel array.

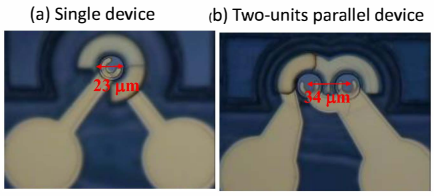

Figure 1. Top-view of demonstrated VCSEL (a) single-unit and (b) two-unit parallel array

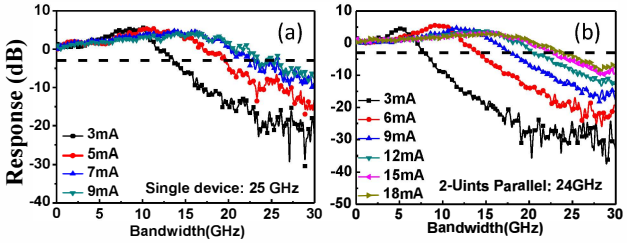

Figure 3. Measured E-O frequency responses of (a) single device and (b) two-units parallel array under different bias currents.

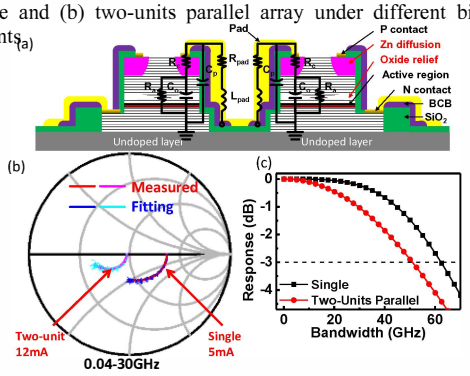

Figure 4. (a) Equivalent-circuit model used for the fitting of S_{11} traces. (b) The measured and fitted S_{11} traces of single and two-unit VCSELs on Smith Chart. (c) The extracted RC-limited frequency responses of single and two-unit VCSEL array.

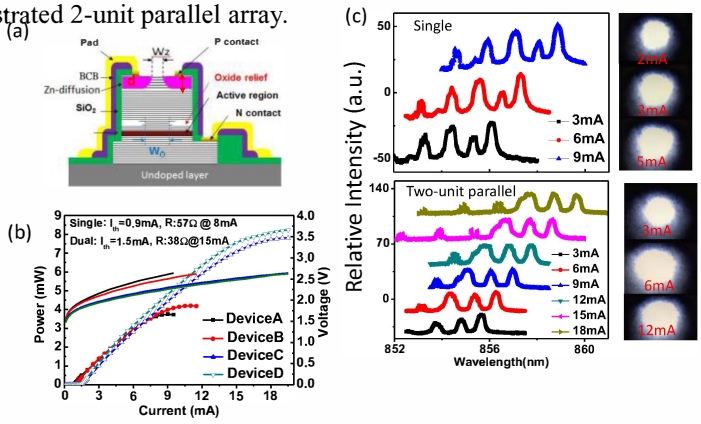

Figure 2. (a) Conceptual cross-sectional views of demonstrated single VCSELs ($W_z/W_\bullet$/d=8/4/1 μm). (b) Measured L-I-V curves of single VCSEL (devices A and B) and two-units parallel (devices C and D). (c) Measured bias dependent optical spectra and corresponding 2-D far-field patterns of single and two-unit parallel devices

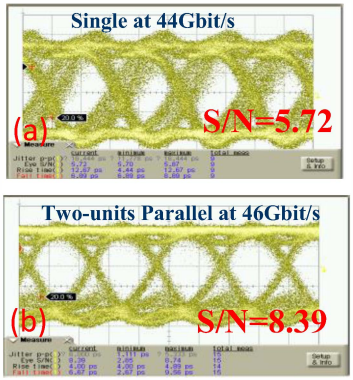

Figure 5. Measured eye-patterns of (a) single device at 44 Gbit/sec and (b) two-unit parallel VCSEL array at 46 Gbit/sec data rates.

V. Reference:

[1] P. Moser, P. Wolf, G. Larisch, H. Li, J. A. Lott, and D. Bimberg, "Energy-efficient oxide-confined high-speed VCSELs for optical interconnects," *Proc. SPIE, Vertical-Cavity Surface Emitting Lasers XVIII*, vol. 9001, pp. 900103, Feb., 2014.

[2] D. M. Kuchta, A. V. Rylyakov, C. L. Schow, J. E. Proesel, C. W. Baks, P. Westbergh, J.S. Gustavsson, and A. Larsson, "A 50 Gb/s NRZ Modulated 850 nm VCSEL Transmitter Operating Error Free to 90 °C," *IEEE/OSA Journal of Lightwave Technology,* vol. 33, no. 4, pp. 802-810, Feb., 2015.

[3] Kai-Lun Chi, Yi-Xuan Shi, Xin-Nan Chen, Jason (Jyehong) Chen, Ying-Jay Yang, J.-R Kropp, N. Ledentsov Jr., M. Agustin, N.N. Ledentsov, G. Stepniak, J. P. Turkiewicz, and Jin-Wei Shi, "Single-Mode 850 nm VCSELs for 54 Gbit/sec On-Off Keying Transmission Over 1 km Multi-Mode Fiber," *IEEE Photon. Technol. Lett.,* vol. 28, no. 12, pp. 1367-1370, June, 2016.

[4] K. Szczerba, P. Westbergh, J. Karout, J. S. Gustavsson, Å. Haglund, M. Karlsson, P. A. Andrekson, E. Agrell, and A. Larsson, "4-PAM for High-Speed Short-Range Optical Communications," *J. Opt. Comm. Netw.*, vol., 4, pp. 885-894, Nov., 2012.

[5] R. Safaisini, J. R. Joseph, and K. L. Lear, "Scalable High-CW-Power High-Speed 980-nm VCSEL Arrays," *IEEE J. of Quantum Electronics,* vol. 46, pp. 1590-1596, Nov., 2010.